Workability Behavior of Aluminium Hybrid Composites(P/M)

P P Shantharaman[1, a *], M Prabhakar[2,b]

[1]Associate Professor, Mechanical Engineering.

Kings College of Engineering, Pudukottai, Tamilnadu, India.

[2]Professor, Mechanical Engineering.

TRP Engineering College, Irungalur Thichy, Tamilnadu, India.

[a]ppshantharaman@yahoo.c.in, [b]mprabha2000@rediffmail.com

Keywords: Upsetting, Triaxial stress, Formability stress index, Stress ratio parameter, Workability.

Abstract. Workability is a degree of the amount of deformation that a powder metallurgy bits and pieces can survive prior to fracture occurred in the forming or upsetting process. Ductile fracture is the most general mode of breakdown in bulk forming process. The formability is a complicated happening, dependent upon the method as well as the material parameters. An investigational research work was performed for the kind of the working behavior of Al–SiC-Y2O3 hybrid composite under triaxial stress state circumstance. Upsetting of Al–SiC–Y2O3 powder metallurgy compacts with various aspect ratios and initial preform densities were carried out and the working behavior of the powder compacts at various state conditions was computed. In the powder metallurgy technique cold pressing can be used for compaction of the reinforcement of SiC and Y2O3 with Aluminum hybrid composites (Al+SiC+Y2O3). The bottle green compacts can be sintered and workability characteristics can be studied. In the hybrid composites, SiC content has been different from 0% to 20% with different particle sizes namely 60 and 80μm. Y2O3 nanoparticles of size 30-50nm and reinforced with 1wt% , 2wt% and 3wt%. The experimental Results can be analyzed for workability and frictional stress state conditions during upsetting as a role of relative density. The formability stress index values obtained for various addition of SiC and Y2O3.

Introduction

Powder metallurgy (P/M) is an extremely developed method of manufacturing accurate metal parts. Over the last seven decades, the technology has matured from making self-lubricating bearings for autos to complex carrier gear set in automobile transmissions and high strength powder-forged connecting rods in engines. P/M technology includes the basic steps: mixing of elemental powders, compaction and sintering or heating the shape in a controlled atmosphere furnace to bond the particles together metallurgically. In the development of new aerospace alloys based on aluminium, titanium and other alloys, P/M technique plays a predominant role [1]. P/M products are widely used from the automotive industry through to aerospace, ordnance, power tool, electronics, business machines, household appliances, garden equipment and much more. This success is due to the advantages of the process which offers over other metal forming technologies such as forging and extrusion; advantages in material utilization, shape complexity and nearest shape dimensional control among others. These, in turn, yield benefits in lower costs and greater versatility [2]

Workability is concerned with the extent to which a material can be deformed in a specific metalworking process without the initiation of cracks. The ductile fracture of the component is the most common mode of failure in any metalworking process. Workability is the complex technological concept that depends upon the ductility of the material and the details of the process parameters. It is the term used to the shaping of materials on various bulk deformation processes like forging, extrusion and rolling, to evaluate the capacity of a material to withstand the induced internal stresses of forming before the splitting of material occurs [3]. Therefore, a complete

description of the workability of a material is specified by its flow stress which depends on processing variables such as strain, strain rate, preheat temperature, die temperature, its failure behavior and the metallurgical transformation that characterize the alloy system to which it belongs.

Mechanical, metallurgical and machinability studies on Al–SiC P/M composites have been done by various authors [4–12]. When the size of the SiC reinforcement of the composite is fine, the degree of cyclic hardening becomes high [13]. The composite materials have a monotonic increase in relative density with pressure [4]. The cyclic stress response of MMCs has strong dependence on the percentage of the reinforcement.

The ductile failure of the Aluminum matrix has been studied for the nucleation, growth and coalescence of voids under tensile load [5]. Studies have revealed that the Al–SiC composite gives better tensile fatigue performance compared to monolithic alloy [14]. Compression deformation test on Al–SiC composite has been carried out at elevated temperature and it has been found that the SiC added Aluminum powder metallurgy composite gives better formability compared to pure Aluminum and proved thro FEM technique [15].

Workability criterion of P/M compacts have been discussed by Abdel-Rahman and El-Sheikh [16], investigating the effect of relative density on the criteria forming limit of P/M compacts during upsetting also. They have proposed the criteria called formability stress index (b) for describing the effect of the mean stress and the effective stress with the help of two theories, proposed by Kuhn-Downey and Whang-Kobayashi.

Narayanasamy et al. [17] presented some of the important criteria generally used for the prediction of workability. Narayanasamy et al. [18] have done more experimental work on workability behavior of Aluminum–Iron composites namely, Al–Al2O3 [19], Al–Fe [20,21], Fe [22], Fe–TiC [23,24] and Fe–C [24] composite during cold upsetting. The same author analyzed the workability of Fe and Fe–TiC under hot forging [22,25–27] technique also.

One of the chief characteristics of the plastic deformation of metals is the fact that the shear stress required to produce slip intermittently increases with increasing shear strain [28]. The strain hardening is a phenomena of slip caused by the previous plastic deformation which in turn is caused by dislocations interacting with each other. Narayanasamy et al. [29,30] performed the work on the strain hardening behavior of the powder metallurgy composites. They evaluated the work hardening characterirstics of sintered Al–Al2O3 [31,32] and Al–Fe [29,33,34] composites preform under uniaxial, plane and triaxial stress state conditions.

In this paper, a complete investigation on the workability criteria of Aluminum and Al–SiC-Y_2O_3 powder preforms was made during cold upsetting. Powder metallurgy preforms with various percentages and aspect ratios were discussed for studying the behavior of workability during cold upsetting under triaxial stress state condition. Literature dealing with the effect of various percentage on the workability under triaxial stress state condition on Al–Glass composite is not available. The present investigation is an attempt to evaluate the effect of the percentage on the workability parameter under triaxial stress state condition.

Nomenclature

F   force applied on the cylindrical preform for deformation(N)
H_o initial height of the cylindrical perform(mm)
H_f height of the barreled cylinder after deformation (mm)
D_o initial diameter of the perform (mm)
D_B bulged diameter of the preform after deformation (mm)
D_{Tc} top contact diameter of the preform after deformation (mm)
D_{Bc} bottom contact diameter of the preform after deformation (mm)
α   Poisson's ratio
σ_z true stress in the axial direction (MPa)
σ_θ true stress in the hoop direction (MPa)

σ_r	true stress in the radial direction (MPa)
σ_{eff}	effective stress (MPa)
σ_m	hydrostatic stress (MPa)
σ	true stress (MPa)
ε	true strain
ε_z	true strain in the axial direction
ε_0	true strain in the hoop direction
ε_r	true strain in the radial direction
β	formability Stress Index
ρ_o	initial preform density of the perform (g/cc)
ρ_f	density of the preform after deformation(g/cc)
ρ_{th}	theoretical density of the fully dense material (g/cc)
$\sigma_{\theta/reff}$	stress ratio parameter
ε_m	true mean strain
h_o/D_o	aspect ratio

Experimental Details

A. Compact preparation: Atomized aluminium powder of 10 µm was procured from M/s. Metal Powder Company Ltd., Madurai, Tamil Nadu, India and analyzed for its purity. The same was found to be 99.7% and insoluble impurities to be 3%. The characterization of aluminium powder was studied by determining the flow rate, apparent density and particle size distribution and these details are provided in Table I.

Powder mix corresponding to Al-various percentage of SiC (different particle sizes namely 60 and 80µm) and Yttrium oxide (particle size of 30-50nm) were blended for all combinations on a pot mill to obtain a homogeneous powder blend. The weight percentage of SiC varied from 0 to 20 % with an interval of 4 % and weight percentage of yttrium oxide varied from 1%,2% and 3%. Cylindrical cold green compacts of various percent of hybrid composite of the above said blend were prepared using a suitable die assembly set. The die set assembly was made out of High Carbon High Chromium Steel (Figure 1). Zinc-stearate was used as lubricant and applied on the inner surface of the die, outer surface of the punch and the top surface of the butt so as to avoid sticking of powder to these surfaces. A known weight of powder was taken and poured in to the die with its butt inserted at the bottom and then the punch was introduced from the top of the die. Green compacts (cylindrical in shape) of the powder blend was prepared on a 1.0 MN capacity hydraulic press using suitable punch and die assembly as shown in Figure 2. The compacting pressure applied was 520MPa, which was maintained for all composition of Al–SiC-Y_2O_3 Hybrid composites.

TABLE I
CHARACTERISTICS OF ALUMINIUM POWDER.

Sieve size [µm]	Percentage distribution [weight]
+106	00.26
+90	02.54
+75	14.73
+63	17.58
+53	24.86
+45	12.33
+38	06.27
−38	21.42
Apparent density (gcm−3)	1.03
Flow rate (by Hall flow meter)	32.00

After compaction, the ejection of green compact was done by removing the butt and placing the die on two parallel blocks of the same height leaving a hole right in the centre of the free space between the two blocks and then applying pressure by means of hydraulic press. The damage to the compact was avoided by given that cotton under the compact. Thus when the punch started moving down through the die cavity, the compact came down in between the space provided by arranging the supporting blocks. The ejection load of the lower order suggested that there was very little sticking of the powder with the die and the punch surfaces. The free surfaces of the green compacts were first coated before sintering with an indigenously developed ceramic mixture [20] and dried under room-temperature condition for a period of 10 hours. Then, second coating was applied at a direction of 90º to the direction of first coating and was allowed to dry for a further period of 10 hours under the same condition as stated above.

B. Sintering: Sintering of powder sequentially involves the establishment and growth of bonds between the particles of powder at their areas of contact and migration of the grain boundaries formed at the bonds. This resulted in spheroidization of the pores between the particles and the elimination of small pores. As the sintering temperature increases, porosity decreases and shrinkage increases [35]. Here, in the present case, the shrinkage was less because the sintering temperature (605ºC) was lower. Bonds formed between the particles during sintering and the number of particle bonds increase as the temperature increases. The ceramic-coated green compacts were sintered in an electric muffle furnace in the temperature range of 605ºC for a sintering time of 120 minutes and allowed to get cooled to room temperature in the furnace itself.
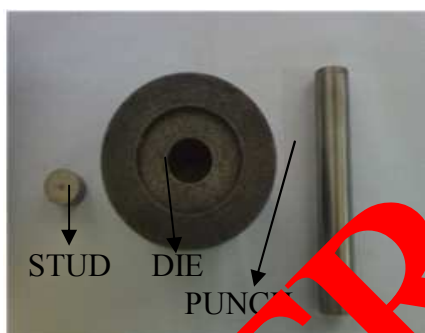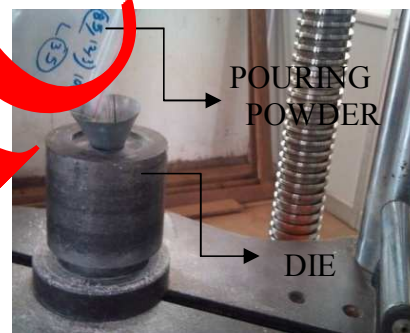

Fig.1 Shows Stud, Die, and Punch

Fig.2 Pouring powder into Die

C. Energy dispersive X-ray spectroscopy (EDAX) analysis: Figure 3 shows the presence of Silicon carbide, alumina and yttria particles in the provided sample. These EDAX facilities were availed of from Central Electrochemical Research Institute, Karaikudi, Tamil Nadu, India, using SEM model HITACHI S-3000H. Higher magnification was used for the present study.

D. Deformation test: Initial diameter (Do), initial height (ho) and the initial perform relative density (ρ_o) of the specimen were measured and recorded. Each compact was subjected to the incremental compressive loads of 0.01 MN and the upsetting was carried between two flat, mirror finished open dies on a hydraulic press of 1.0 MN capacity. The deformation was carried out until the appearance of first visible crack was noticed on the free surface. After each interval of loading, dimensional changes in the specimen such as height after deformation (h_f), top contact diameter (D_{TC}), bottom contact diameter (D_{BC}), bulged diameter (D_B) and density of the preform (ρ_f) were measured. The schematic diagram showing the various parameters measured before and after deformation is provided in Fig. 4. Using the Archimedes principle, the density of upset performs was also determined after every loading interval. The deformation tests were continued until the fracture occurred at outer surface of the specimen.
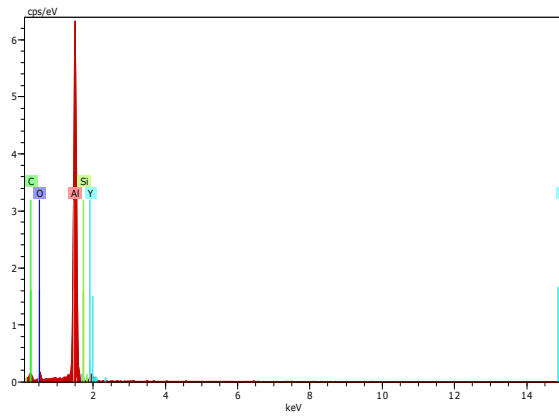
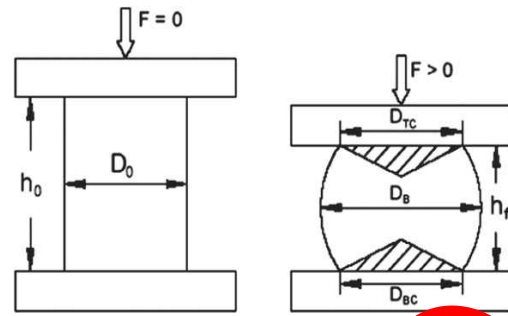Fig.3 Elemental (EDAX) Analysis for Al – 4% SiC –1% Y_2O_3 Hybrid Composite.

Fig. 4 Upset test preform before and after deformation.

Theoretical Investigations

The various upsetting parameters under triaxial stress state condition are determined with the application of the following expressions.

A. Stress: The state of stress in a triaxial stress condition is given by Narayanasamy et al. [34] as follows:

$$\alpha = [(2+R^2)\sigma_\theta - R^2(\sigma_z + 2\sigma_\theta)] / [(2+R^2)\sigma_z - R^2(\sigma_z + 2\sigma_\theta)]$$

From the Eq. (1) for the known values of poisson ratio (α), relative density (R) and true axial stress (σ_z), the true hoop stress component (σ_θ) can be determined as follows:

$$\sigma_\theta = \{[(2\alpha + R^2)] / (2 - R^2 + 2R^2\alpha)]\} \sigma_z$$

At triaxial stress state condition, the relative density (R) of the compacts plays a vital role in the determination of the true hoop stress component (σ_θ). The true hydrostatic stress is given by,

$$\sigma_m = [(\sigma_r + \sigma_z + \sigma_\theta) / 3]$$

Since $\sigma_r = \sigma_\theta$ in the case of axisymmetric triaxial stress condition, the above equation becomes as follows:

$$\sigma_m = [(\sigma_z + 2\sigma_\theta) / 3]$$

The true effective stress can be determined from the following expression in terms of cylindrical coordinates explained elsewhere[36]

$$\sigma^2_{eff} = \{[\sigma^2_z + \sigma^2_\theta + \sigma^2_r - R^2(\sigma_z\sigma_\theta + \sigma_\theta\sigma_r + \sigma_z\sigma_r)] / [2R^2 - 1]\}$$

Since $\sigma_r = \sigma_\theta$ for cylindrical axisymmetric upsetting operation, the true effective stress is determined as follows:

$$\sigma_{eff} = \{[\sigma^2_z + 2\sigma^2_\theta - R^2(\sigma_z\sigma_\theta + \sigma^2_\theta + \sigma_z\sigma_\theta)] / [2R^2 - 1]\}^{1/2}$$

B. Formability stress index: As an evidence of experimental examination implying the importance of the spherical component of the stress state on fracture, a Vujovic and Shabaik [37] proposed a parameter called a Formability Stress Index 'β' is given by,

$$\beta = [3\sigma_\theta / \sigma_{eff}]$$

This index determines the fracture limit as explained in Ref.[16].

C. *Strain*: The true axial strain (ε_z) is expressed as

$$\varepsilon_z = \ln [\, h_o / h_f \,]$$

The true hoop strain (ε_0) can be determined by the following expression as described elsewhere [36].

$$\varepsilon_0 = \ln [\, (2D^2{}_b + D^2{}_c) / 3D^2{}_0 \,]$$

Result and Discussion

A. Workability behavior of stresses on Al–SiC-Y2O3 hybrid composite Perform

Fig. 5a–5d has been plotted between various triaxial stresses namely the true axial stress (σ_z), the true hoop stress (σ_θ), the true effective stress (σ_{eff}), the true mean stress (σ_m) and true axial strain (ε_z) for Aluminum contains various percentages of SiC and Y_2O_3.
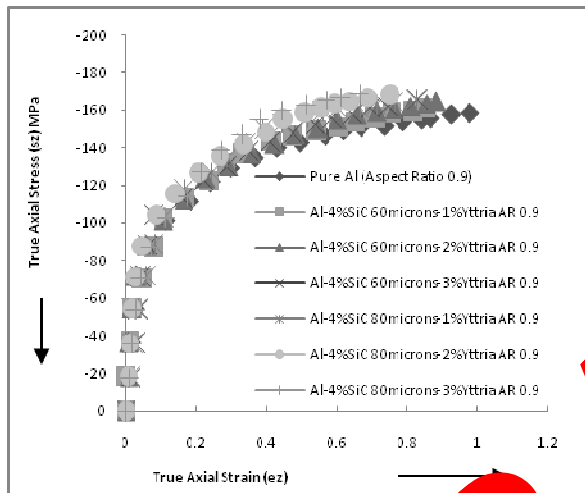

Fig.5a. The variation of true axial stress with respect to true axial strain of Hybrid composite with AR 0.9
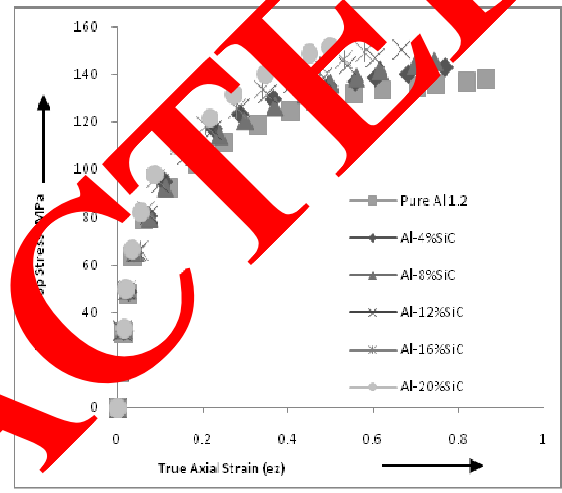

Fig.5b. The variation of true hoop stress with respect to true axial strain of Hybrid composite with AR 1.2 with 1% Yttria
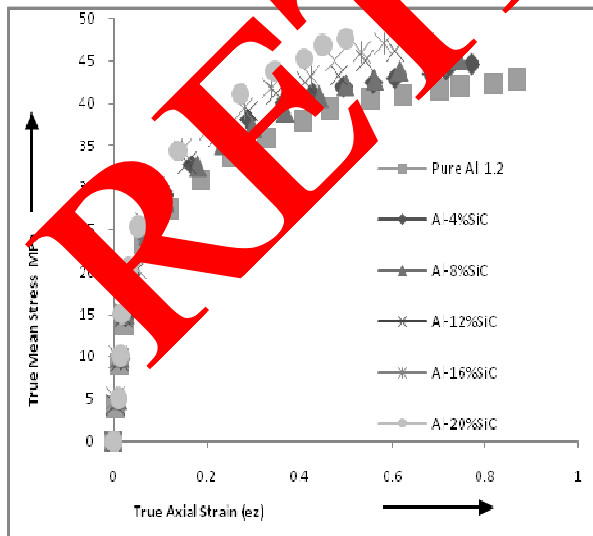

Fig.5c. The variation of true mean stress with respect to true axial strain of Hybrid composite with AR 1.2 with 1% yttria
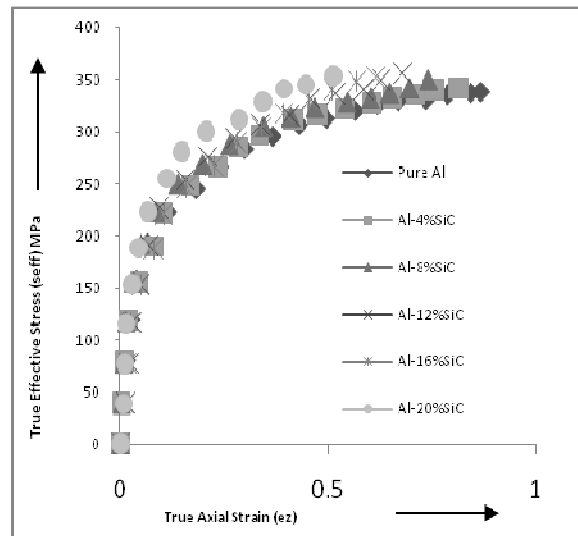

Fig.5d. The variation of true effective stress with respect to true axial strain of Hybrid composite with AR 0.9 with 1% yttria.

It is observed that the true axial stress (σ_z) increases with increasing amount of SiC added in the Al–SiC-Y_2O_3 composite. From these figures it is understood that the true axial stress (σ_z) and other stresses namely the true hoop stress (σ_θ), the true effective stress (σ_{eff}), and the true mean stress (σ_m), are affected by the amount of SiC content and Y_2O_3 content. The same behavior has been observed when stresses namely the true hoop stress (σ_θ), the true effective stress (σ_{eff}) and the true mean stress (σ_m), are plotted against the true axial strain (ε_z). As SiC content increases the porosity level decreases and the relative density increases for the same compacting pressure. This may be one of the reasons for the increasing stresses for higher amount of SiC content. Further, with the increase of SiC content, the SiC particulates impede the motion of dislodgment and hence the stress required for further deformation increases. Due to these reasons all stresses increase with increasing amount of Silicon carbide.

B. Workability behavior of formability stress index(β) on Al–SiC-Y2O3 hybrid composite Perform

Fig.6a-6b has been plotted between the relative density and the formability stress index for the upsetting of Al–SiC-Y_2O_3 powder compacts for the various aspect ratios and two different particle size of SiC under triaxial stress state condition. It is observed that the formability stress index varies with aspect ratio, particle size of SiC and various percentages of SiC. For the lower aspect ratio and higher initial preform density, the stress formability stress index takes a very high value. For compacts of higher aspect ratio and lower initial fractional preform density, the stress formability index value moves closer to the minimum value. Table II provides the maximum value of the formability index (b) for various SiC percentage addition tested in the Al–SiC-Y_2O_3 composites. It is observed that as the SiC content increases, the formability stress index (β) also increases to a very high value because of better densification due to greater amount of load transfer rate to the Aluminum matrix by SiC percentage.
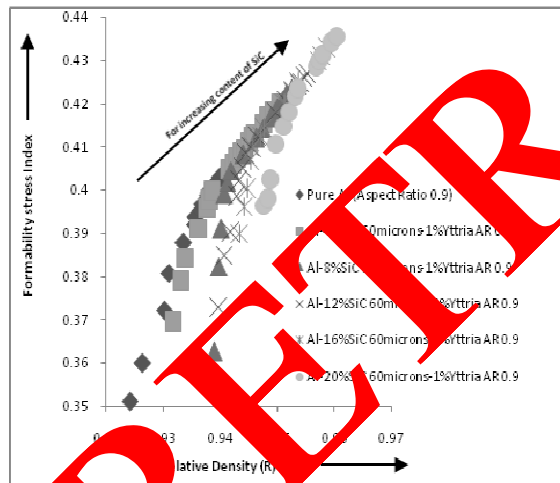

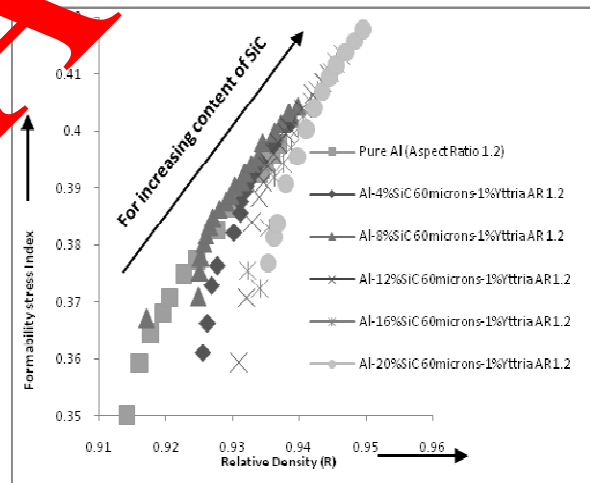Fig.6a. The variation of formability stress index (β) with respect to the relative density (R) AR 0.9

Fig.6b. The variation of formability stress index (β) with respect to the relative density (R) AR 1.2

The value of maximum formability stress index (β) for various Yttria content in composites are tabulated in Table III. The reason may be attributed to the fact that the pore size decreases with increasing addition of Yttria as that higher amount of load may be transferred by the Yttria to the Aluminum matrix. Here, better densification can be achieved for the higher addition of Yttria. The reason is that as the Yttria content increases, the relative density also increases and porosity decreases.

The higher addition of Yttria in Aluminum matrix reduces the pore size. Smaller is the pore size, higher is the mean stress value. This may be the reason that the formability stress index (β)

increases with increasing amount of Yttria content. This result is in good agreement with the findings of Narayanasamy et al. as described elsewhere [38].

TABLE II
THE VALUES OF MAXIMUM FORMABILITY STRESS INDEX FOR VARIOUS SIC CONTENTS AND 1%YTTRIA

Sl. no.	Percentage addition of SiC	Maximum formability stress index [β]			
		Aspect ratio 0.9		Aspect ratio 1.2	
		SiC particle size 60μm	SiC particle size 80μm	SiC particle size 60μm	SiC particle size 80μm
1	Pure Al	0.4105		0.3978	
2	4% SiC	0.420	0.424	0.401	0.408
3	8% SiC	0.421	0.429	0.404	0.4?0
4	12% SiC	0.427	0.436	0.409	0.41?
5	16% SiC	0.432	0.441	0.4??	0.416
6	20% SiC	0.435	0.445	0.417	0.421

TABLE III
THE VALUES OF MAXIMUM FORMABILITY STRESS INDEX FOR VARIOUS YTTRIA CONTENTS AND ?SIC

Sl. no.	Percentage addition of Yttria	Maximum formability stress index [β]			
		Aspect ratio 0.9		Aspect ratio 1.2	
		SiC particle size 60μm	SiC particle size 80μm	SiC particle size 60μm	SiC particle size 80μm
1	Pure Al	0.4105		0.3978	
2	1%Yttria	0.420	0.424	0.420	0.424
3	2%Yttria	0.427	0.429	0.416	0.419
4	3%Yttria	0.429	0.432	0.424	0.426

C. Workability behavior of stress ratio parameter on Al–SiC-Y2O3 hybrid composite Performance

However, when the stress ratio parameter (σ_m/σ_{eff}) is plotted against the relative density (R) for Aluminum containing five different SiC(two different particle size) percentages, two different aspect ratios and three different yttria percentages as in Fig. 7a-7b.

As the SiC content increases, the negative slope value also increases because Al–SiC-Y$_2$O$_3$ composite exhibits fine pores compared to pure Aluminum. Because of this, the stress ratio parameter (σ_z/σ_m) decreases with increasing SiC content. The reason is the true axial stress (σ_z) that is compressive in nature. The values of maximum stress ratio parameter (σ_m/σ_{eff}) for variation of SiC contents in composites are tabulated in Table IV, and the maximum values of stress ratio parameter (σ_m/σ_{eff}) for variation of yttria contents in composites are tabulated in Table V.
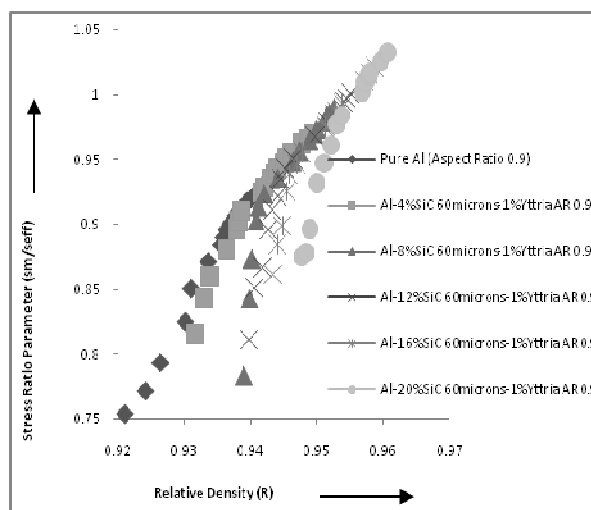
Fig.7a. The variation of stress ratio parameter (σ_m/σ_{eff}) with respect to the relative density(R) AR0.9(60µm)
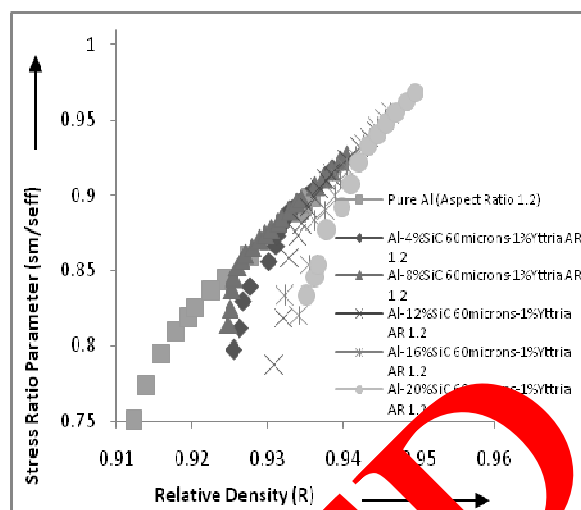

Fig.7b. The variation of stress ratio parameter (σ_m/σ_{eff}) with respect to the relative density(R) AR1.2(60µm)

TABLE IV
THE VALUES OF MAXIMUM STRESS RATIO PARAMETER (Σ_M/Σ_{EFF}) FOR VARIOUS SIC CONTENTS AND 1% YTTRIA

Sl. no.	Percentage addition of SiC	Maximum stress ratio parameter [σ_m/σ_{eff}]			
		Aspect ratio 0.9		Aspect ratio 1.2	
		SiC particle size 60µm	SiC particle size 80µm	SiC particle size 60µm	SiC particle size 80µm
1	Pure Al	0.945		0.904	
2	4% SiC	0.977	0.989	0.9162	0.938
3	8% SiC	0.983	1.007	0.925	0.942
4	12% SiC	0.996	1.033	0.942	0.954
5	16% SiC	1.02	1.047	0.953	0.967
6	20% SiC	1.03	1.062	0.968	0.976

TABLE V
THE VALUES OF MAXIMUM STRESS RATIO PARAMETER (Σ_M/Σ_{EFF}) FOR VARIOUS YTTRIA CONTENTS AND 4%SIC

Sl. no.	Percentage addition of Yttria	Maximum stress ratio parameter [σ_m/σ_{eff}]			
		Aspect ratio 0.9		Aspect ratio 1.2	
		SiC particle size 60µm	SiC particle size 80µm	SiC particle size 60µm	SiC particle size 80µm
1	Pure Al	0.945		0.904	
2	1%Yttria	0.977	0.989	0.9162	0.938
3	2%Yttria	1.001	1.011	0.964	0.974
4	3%Yttria	1.008	1.017	0.9909	0.997

Conclusions

The following conclusions can be drawn from the above results and discussions.

The addition of higher SiC content as reinforcement in the Aluminum matrix increases the strength property, because of reduction in pore size or increase in relative density. In general, the formability stress index (β) increases with increasing addition of SiC because the pore size decreases and the geometric work hardening would be lesser.

The formability stress index (β) increases with increasing addition of yttria because of better densification and decrease in pore size.

80μm size SiC added composites show higher formability stress index value (β) compared to other particle size added composite because of better densification due to better load transfer rate of SiC to the aluminium matrix compared to smaller particle size.

The stress ratio parameter (σ_m/σ_{eff}) is found to be higher for Al–SiC-Y_2O_3 composites compared to pure aluminium because of better densification.

The stress ratio parameter (σ_z/σ_m) decreases in the case of Al–SiC-Y_2O_3 composite compared to pure aluminium because of fine pore size associated with high hydrostatic stress (σ_m).

For performs with higher percentage addition of SiC,or yttria the initiation of crack exhibits at lower fracture strain.

Acknowledgment

References

[1]   D.B. Miracle, Compos. Sci. Technol. 65 (2005) 2526–2540..

[2]   ASM Handbook on Powder Metal Technologies and Applications, ASM International, USA, 1984.

[3]   ASM Metals Handbook on Forming, ASM International, USA, 1984.

[4]   Sridhar I, Fleck NA. Yield behavior of cold compacted composite powders. Acta Mater 2000;48:3341–5.

[5]   [4] Lu YX, Hung XM, Lee CS, Li RKY, Huang CG, Lai JKL. Microstructure and mechanical behavior of SiC particles reinforced aluminum composite under dynamic loading. J Mater Process Technol 1999;94:175–8.

[6]   Dumont, Baptiste D, Guedra-degeorges D, Foalquter J. Multiscale modeling of the damaged plastic behavior and failure of Al/SiCp composites. Int J Plastic 1999;15:667–85.

[7]   Cadek J, Zhu SJ, Milic'ka K. Creep behaviour of ods-aluminium reinforced by silicon carbide particulates: ods Al– 30 SiCp composite. Mater Sci Eng A 1998;248:65–72.

[8]   Pan YB, Qlu JH, Morita M. Oxidization and micro hardness of SiC–AlN composite at high temperature. Mater Res Bull 1998;33(1):133–9.

[9]   Li Y, Mohamed FA. An investigation of creep behavior in a SiC–2124 Al composite. Acta Mater 1997;45(11):4775–85.

[10]   Geiger AL, Hasselman DPH, Weich P. Electrical and thermal conductivity of discontinuously reinforced aluminum composites at sub-ambient temperatures. Acta Mater 1997; 45(9):3911–4.

[11]   Sivakumar K, Balakrishna Bhatt T, Ramakrishnan P. Dynamic consolidation of aluminium and Al-20 vol SiCp composite powders. J Mater Process Technol 1996;62:191–8.

[12] Liaw PK, Shannon RE, Clark Jt WG, Harrigan Jt WC, Jeong'p H, Hsu DK, et al. Non-destructive characterization of material matrix composites properties of metal, South Korea. Mater Chem Phys 1995;39:220–8.

[13] Varma Vijay K, Kumar SV, Mahajan YR, Kutumbara VV. Cyclic stress response of Al–Cu–Mg alloy matrix composites with SiCp of varying sizes. Scripta Mater 1998;38(10):1571

[14] Huang ZW, Mccoll IR, Harris SJ. Mater Sci Eng A   1996;215:67–72.

[15] Szczepanik S, Lohnert W. The formability of the Al–5% SiC composite obtained using P/M method. J Mater Process Technol 1996;60:03–709.

[16] Abdel-Rahman M, El-Sheikh MN. Workability in forging of powder metallurgy compacts. J Mater Process Technol 1995;54:97–102.

[17] Narayanasamy R, Ponalagusamy R, Subramanian KR. Generalized yield criteria of porous sintered powder metallurgy metals. J Mater Process Technol 2001;110:182–5.

[18] Narayanasamy R, Ramesh T, Pandey KS. An investigation on instantaneous strain hardening behavior in three dimensions of aluminum–iron composites during cold upsetting. Mater Sci Eng A 2005;394:149–60.

[19] Narayanasamy R, Ramesh T, Pandey KS. Workability studies on cold upsetting of Al–Al2 O3 composite material. J Mater Des 2006;27:566–75.

[20] Narayanasamy R, Ramesh T, Pandey KS. Some aspects on workability of aluminum–iron powder metallurgy composite during cold upsetting. Mater Sci Eng A 2005;391:418–26.

[21] Selvakumar N, Narayanasamy R. Deformation behavior of cold upset forming of sintered Al–Fe composite performs. J Eng Mater Technol 2005;127:251–6.

[22] Narayanasamy R, Senthilkumar V, Pandey KS. Some aspects on hot forging features of P/M sintered iron performs under various stress state condition. Mech Mater 2006;38:367–86.

[23] Narayanasamy R, Senthilkumar V, Pandey KS. Some aspects of workability studies on P/M sintered high strength 4% titanium carbide composite steel performs during cold upsetting. J Mater Des 2006;3:39–57.

[24] Narayanasamy R, Ananthakrishnan V, Pandey KS. Effect of carbon content on workability of powder metallurgy steels. Mater Sci Eng 2008;44:337–42.

[25] Narayanasamy R, Senthilkumar V, Pandey KS. Some aspects of workability studies on hot forging of sintered high strength 4% Titanium Carbide composite steel performs. J Mater Sci EngA 2006;425:121–30.

[26] Narayanasamy R, Senthilkumar V, Pandey KS. Some aspects of workability studies on sintered high strength P/M Steel composite performs of varying TiC contents during hot forging. J Mater Sci Eng 2008;43:102–16.

[27] Narayanasamy R, Senthilkumar V, Pandey KS. Some aspects on hot forging features of P/M sintered high-strength titanium carbide composite Steel performs under different stress state conditions. J Eng Mater Technol 2007;129:113–29.

[28] Dieter GE. Mechanical metallurgy. New York: McGraw-Hill; 1988.

[29] Narayanasamy R, Ramesh T, Pandey KS. An investigation on instantaneous strain hardening behavior in three dimensions of aluminum–iron composites during cold upsetting. J Mater Sci Eng A 2005;394:149–60.

[30] Narayanasamy R, Pandey KS. Phenomenon of barreling in aluminum solid cylinders during cold upset – forging. J Mater Process Technol 1997;70:17–21.

[31] Narayanasamy R, Ramesh T, Pandey KS. An experimental investigation on strain hardening behaviour of Aluminium–3.5% Alumina powder metallurgy composite perform under various stress states during cold upset forming. J Mater Des 2007;28:1211–23.

[32] Narayanasamy R, Ananthakrishnan V, Pandey KS. Comparison of workability strain and stress parameters of powder metallurgy Steels AISI 9840 and AISI 9845 during cold upsetting. J Mater Des 2008;29:1919–25.

[33] Narayanasamy R, Selvakumar N, Pandey KS. Phenomenon of instantaneous strain hardening behavior of sintered Al–Fe composite performs during cold axial forming. J Mater Des 2007;28:1358–63.

[34] Narayanasamy R, Ramesh T, Pandey KS. Some aspects on strain hardening behavior in three dimensions of aluminum–iron powder metallurgy composite during cold upsetting. J Mater Des 2006;27:640–50.

[35] Production and sintering practices in powder metal technologies and Applications. ASM Hand Book, vol. 07. ASM International; 2002. p. 468–503.

[36] Narayanasamy R, Ramesh T, Pandey KS. Effect of particle size   on   new   constitutive relationship of aluminum–iron powder metallurgy composite during cold upsetting. J Mater Des 2008;29:1011–26.

[37] Vujovic V, Shabaik AH. A new workability criteria for ductile metals. J Eng Mater Technol 1986;108(3):245–9.

[38] Narayanasamy R, Ramesh T, Prabhakar M. Effect of particle size of SiC in aluminum matrix on workability and strain hardening behavior of P/M composite. J Mater Sci Eng A 2009;504:13–23.